Current Alzheimer Research, 2023, *20*, 11-28

RESEARCH ARTICLE

Alpha Rhythm Wavelength of Electroencephalography Signals as a Diagnostic Biomarker for Alzheimer's Disease

Lingfeng Liu[1#], Lijun Hao[2#], Qian Yang[1], Qing Cao[2], Nan Jiang[3] and Meiyun Zhang[2,*]

[1]*Tianjin Union Medical Center, Tianjin Medical University, Tianjin, China;* [2]*Department of Neurology, Tianjin Union Medical Center, Tianjin, China;* [3]*School of Mechanical Engineering, Tianjin University, Tianjin, China*

Abstract: ***Objective*:** To explore changes in the alpha rhythm wavelength of background electroencephalography in Alzheimer's disease patients with different degrees of dementia in a resting state; examine their correlation with the degree of cognitive impairment; determine whether the alpha rhythm wavelength can distinguish mild Alzheimer's disease patients, moderately severe Alzheimer's disease patients, and healthy controls at the individual level; and identify a cut-off value to differentiate Alzheimer's disease patients from healthy controls.

***Methods*:** Quantitative electroencephalography signals of 42 patients with mild Alzheimer's disease, 42 patients with moderately severe Alzheimer's disease, and 40 healthy controls during rest state with eyes closed were analyzed using wavelet transform. Electroencephalography signals were decomposed into different scales, and their segments were superimposed according to the same length (wavelength and amplitude) and phase alignment. Phase averaging was performed to obtain average phase waveforms of the desired scales of each lead. The alpha-band wavelengths corresponding to the ninth scale of the background rhythm of different leads were compared between groups.

***Results*:** The average wavelength of the alpha rhythm phase of the whole-brain electroencephalography signals in Alzheimer's disease patients was prolonged and positively correlated with the severity of cognitive dysfunction ($P < 0.01$). The ninth-scale phase average wavelength of each lead had high diagnostic efficacy for Alzheimer's disease, and the diagnostic efficacy of lead P3 (area under the receiver operating characteristic curve = 0.873) was the highest.

***Conclusion*:** The average wavelength of the electroencephalography alpha rhythm phase may be used as a quantitative feature for the diagnosis of Alzheimer's disease, and the slowing of the alpha rhythm may be an important neuro-electrophysiological index for disease evaluation.

ARTICLE HISTORY

Received: November 12, 2022
Revised: February 19, 2023
Accepted: March 09, 2023

DOI:
10.2174/1567205020666230503094441

Keywords: Alzheimer's Disease, EEG, alpha rhythm, alpha-band wavelength, average phase waveform, wavelet transformation.

1. INTRODUCTION

Alzheimer's disease (AD) is a chronic progressive neurodegenerative disease characterized by impairments in memory function and numerous other cognitive domains [1-3]. It is the primary cause of senile dementia and accounts for approximately 70% of all dementia patients [4-6]. The typical pathological feature of AD is the formation of extracellular neuritic plaques containing β-amyloid (Aβ) and tau-containing neurofibrillary tangles in cells, eventually leading to synaptic and neuronal apoptosis [1, 7, 8]. At present, the most effective method for the diagnosis of AD is the detection of a decrease in the cerebrospinal fluid (CSF) biomarker Aβ42 and an increase in phosphorylated tau protein (p-TAU 181) [9-12]. Fluorodeoxyglucose-positron emission tomography measures the region and degree of cerebral hypometabolism, reflecting the clinical severity of AD [1, 9]. Although CSF and imaging examinations have high diagnostic value, their invasiveness, exposure to radiation, and high-cost limit their clinical application. To date, several studies have shown that the Aβ42/Aβ40 ratio in peripheral blood [1, 9] and p-TAU 181 detection have great significance in the diagnosis of AD [13-15]; however, their reliability is significantly lower than that of CSF biomarkers [1]. A recent study conducted in the United States has suggested that the pathological process of AD begins with the dysfunction of autophagic lysosomal acidification in nerve cells, leading to the metabolic disorder of Aβ and its precursor proteins, which gradually disintegrates lysosomes and cells and results in the formation of neuroinflammatory plaques alongside the remains of nerve cells and Aβ. The theory that cell death precedes the formation of extracellular amyloid plaques has been proposed [16], which challenges traditional neuropathophysiological concepts and indicates that brain cell necrosis

*Address correspondence to this author at the Department of Neurology, Tianjin Union Medical Center, Tianjin, 300121, China; Tel: 022-27557009; E-mail: zmy22202@aliyun.com

[#]*These authors contributed equally to this work.*

1875-5828/23 $65.00+.00

has already occurred when pathological biomarkers are detected. This may reshape the direction of the pathological diagnosis of AD.

Electroencephalography (EEG) is a non-invasive, simple, low-cost, and high-temporal resolution electrophysiological monitoring method [5, 17]. EEG signals reflect changes in the synchronous activity of neurons under spontaneous and stimulation states and can reveal neuronal degeneration and synaptic loss. Changes in EEG signals are closely related to human cognition [4, 5, 17]. Indeed, several studies have observed cognitive impairment in AD patients before the detection of brain tissue atrophy or behavioral symptoms [5]; thus, EEG technology can assist in the diagnosis of early dementia [18]. Recent advances in EEG have suggested that EEG is more sensitive than brain atrophy and brain connectivity maps obtained using functional magnetic resonance imaging (MRI) for detecting the early stages of AD [17] and that it has the potential for the identification of diagnostic biomarkers for dementia.

EEG signals are generally divided into five frequency bands: delta (δ; 2-4 Hz), theta (θ; 4-8 Hz), alpha (α; 8-13 Hz), beta (β; 13-30 Hz), and gamma (γ; 30-40 Hz). In addition, α is further subdivided into α1 (8-10.5 Hz) and α2 (10.5-13 Hz), and β is divided into β1 (13-20 Hz), and β2 (20-30 Hz)[19]. Recent progress in EEG methodologies for the diagnosis of AD in rest state has mainly focused on the slowing of EEG background signals [8, 20, 21] (*e.g.,* the increase of slow wave band power and the decrease of fast wave band power [22, 23]) to evaluate the neurophysiological mechanism underlying cortical arousal and attention state fluctuation disorder in AD patients [24]; complexity reduction [22] (*e.g.,* dynamic characteristic indices, such as Shannon entropy, approximate entropy, sample entropy, permutation entropy, fractal dimension, multi-scale entropy, Lempel Ziv complexity, and Hurst index) to measure reductions in information processing capacity of the brain [20, 25-29]; decreased connectivity [22] (*e.g.,* average phase coherence, phase synchronization degree, synchronization likelihood, phase lag index, and Granger causality) to examine decreases in brain function synchronization [20, 30, 22, 31]. Furthermore, changes in power spectrum and complexity may reflect the dysregulation of neuroplasticity of cortical neural networks in different brain regions [24, 32], which is related to the destruction of functional or structural integrity in AD, such as cholinergic defects in neurons, neuronal loss, and disruption of cortical information transmission between various brain regions [31]. As a result, the synchronous activity of neurons reduces, synchronization and coupling functions become abnormal, and neural activity patterns become simplified, leading to the progression of cognitive dysfunction [20].

Among the various frequency bands, the α band of the background rhythm is the most widely studied [33, 34]. When healthy adults are in a rest state with eyes closed, EEG usually shows an α dominant rhythm in the occipital region [35]. This rhythm is generated by the synchronous activity of thalamic neurons, regulated by the interaction between the thalamic-cortex and cortico-cortex and is closely related to cognitive function [12, 36, 37]. The strength of occipital α-rhythm activity is negatively correlated with gray matter and hippocampal atrophy [35, 38] and positively correlated with scores of cognitive function assessments [36]. In addition, patients with AD and mild cognitive impairment show a shift in power spectrum to a lower frequency band, a decrease in the consistency of the fast rhythm [22], and a decrease in the amplitude of the occipital α rhythm [19]. Moreover, the activity of the δ and θ bands increases, while the activity of the α and β bands decreases [39, 40].

Numerous studies have used the ratio of the combined values of frequency bands to determine the degree of decreased high-frequency activity and increased low-frequency activity. For example, Ozbek *et al.* used decreased α/θ power as an index of decreased α power and increased θ power to distinguish early-onset AD patients from healthy subjects [6]. Several studies have also found that a decrease in (α+β)/(δ+θ) and the α2/α1 ratio are specifically related to cognitive decline and reflect the slowing of EEG activity [4, 41, 42]. Polverino *et al.* reported that the α2/α1 power ratio is lower in patients with mild cognitive impairment than in healthy controls (HC), although the total α power did not differ significantly [43]. It is possible that α1 is mainly related to overall attentional fluctuation, whereas α2 reflects the content of sensorimotor or semantic information in specific nervous system oscillations [36].

Another study on the α rhythm by Babiloni *et al.* found that the α-band connections and functional connectivity between the cerebral hemispheres were significantly reduced in patients with AD and mild cognitive impairment, whereas subjects with intact cognitive function had higher functional connectivity between the hemispheres [17]. These reductions in the patients decreased stepwise with the severity of cognitive decline [44]. Furthermore, a drug study has shown that the α -band global functional connectivity of AD patients improved following cognitive drug therapy [19].

The aim of this study was to develop a new method to identify the key characteristics of α rhythm slowing in AD patients.

2. MATERIALS AND METHODS

2.1. Participants

A total of 84 AD patients from the outpatient and inpatient departments of Tianjin Union Medical Center were included in this study, which comprised 42 mild AD (mAD) patients (21 male, mean age 73.31 ± 9.462 years) and 42 moderately severe AD (msAD) patients (22 male, mean age 67.93 ± 8.148 years).

Inclusion criteria for AD patients were as follows: (1) met diagnostic criteria of the National Institute of Aging and Alzheimer's Disease Association Diagnostic Guidelines Writing Group (2011) [45] ; (2) impairment of two or more cognitive domains in the fields of memory, language, visual space, execution, and changes in personality and behavior; (3) aged over 50 years, with an educational level above primary school education; (4) impairment of activities of daily living (> 22 points on the Abilities of Daily Living Scale [ADL]) caused by a non-somatic structural disorder that seriously affects social function, and a Clinical Dementia Rating Scale (CDR) score of 1-3 points. Patients with a CDR

score of 1 were classified as mAD, and those with a CDR score of 2 or 3 were classified as msAD.

Exclusion criteria were as follows: (1) patients with cognitive impairment caused by frontotemporal dementia, dementia with Lewy bodies, vascular dementia, Parkinson's syndrome, epilepsy, or other mental diseases; (2) patients with serious digestive, respiratory, circulatory, blood, immune, or other system diseases; (3) patients whose cranial computed tomography or MRI showed significant abnormal signals in important regions, such as the frontal lobe, temporal lobe, hippocampus, and thalamus; (4) patients with a history of drug, poison, or alcohol abuse or head trauma.

We recruited 40 HC subjects matched for age and educational level during the same period, comprising 17 male patients with a mean age of 68.53 ± 9.543 years. Inclusion criteria were as follows: (1) normal cognitive function and no complaints of subjective memory loss (defined as a Minimental State Examination [MMSE] score of ≥ 27 points, junior high school and above education, ADL score of < 22 points, CDR score of 0 points); (2) no history of neuropsychiatric disorders or drug and alcohol abuse; (3) no history of serious heart, lung, liver, or kidney-related diseases; (4) no obvious sleep disorder.

Local institutional ethics committees approved the study.

2.2. Neuropsychological Measures

Data on the medical history and medication of AD patients were collected. Participants underwent evaluations using the following scales, which were completed by the participants themselves or by a guardian who was familiar with the participant's condition. The degree of cognitive impairment was assessed using the MMSE and the CDR. The MMSE scale was used to assess global cognitive performance. The ADL was used to assess impairments in daily life. The Chinese versions of the auditory verbal learning test, shape trail test, animal fluency test, clock drawing test, and digital span test were used to evaluate participants' memory, executive function, language ability, spatial-temporal structure, attention, and other cognitive functions. The Hachinski Ischemic Scale was used to calculate the cerebral ischemia index. The Hamilton Depression and Anxiety Scales were used to assess depression and anxiety. Patients whose condition was too severe to cooperate or complete any part of the assessment were recorded as unable to complete, and the score of the patient for the incomplete cognitive assessment was recorded as 0.

2.3. EEG Recording and Analysis

2.3.1. EEG Data Acquisition

Subjects were instructed not to take sleep-disrupting medications (*e.g.,* antipsychotics, antidepressants, benzodiazepines, or any sleep-inducing drugs) or substances (*e.g.,* coffee and alcohol) from 2 days before and on the day of the examination and to wash and dry their hair on the day of the examination. The scalp was cleaned with alcohol before the EEG recording. EEG data were acquired in a quiet and comfortable EEG room. During the EEG recording, subjects were seated in a quiet room and were asked to keep their eyes closed. EB-neuro Be-light (Firenze, Italy) EEG and scalp disc electrodes were used for the EEG recording. We placed 20 scalp electrodes according to the international standard 10-20 system, which included two auricular electrodes. Bilateral auricular electrodes were used as reference electrodes to collect 16-lead EEG signals. The electrical impedance was maintained at < 5 kΩ, the sampling frequency was set to 512 Hz, and low-frequency and high-frequency filtering were set to 0.3 Hz and 35 Hz, respectively. The total recording time was 10-20 minutes. Lead settings were as follows: FP1-A1, FP2-A2, F3-A1, F4-A2, C3-A1, C4-A2, P3-A1, P4-A2, O1-A1, O2-A2, F7-A1, F8-A2, T3-A1, T4-A2, T5-A1, and T6-A2. After EEG data were collected, 20 s 16-lead EEG data without visual artifacts were selected for subsequent analyses.

2.3.2. EEG Digital Signal Analysis

2.3.2.1. Wavelet Analysis

Gauss continuous wavelet transform (CWT) analysis was used to analyze the EEG data. Wavelet transform is a time-frequency localization analysis method which converts one-dimensional unsteady EEG signals into two-dimensional time-frequency signals, gradually refines signals of multiple scales, and enables accurate synchronization analysis in the time and frequency domains. The calculation method is expressed by the following formula:

$$CWTf(\alpha,\beta) = \int_{-\infty}^{+\infty} f(t)\cdot\psi_{\alpha,\beta}(t)dt \qquad (1).$$

The wavelet generating function was transformed by translating the β units and scaling the α units to obtain the wavelet function family $\psi_{\alpha,\beta}(t)$, where t represents time, α represents the scale transformation factor, and β represents the translation parameter corresponding to the time variable t. The translation scaling process is shown in Fig. (**1**). The formula for the wavelet function is as follows in Eq. (2):

$$\psi_{\alpha,\beta}(t) = \frac{1}{\sqrt{\alpha}}\psi(\frac{t-\beta}{\alpha}) \qquad (2)$$

After the Gauss CWT analysis, we determined the corresponding relationship between frequency and scale number, which is shown in Table **1**.

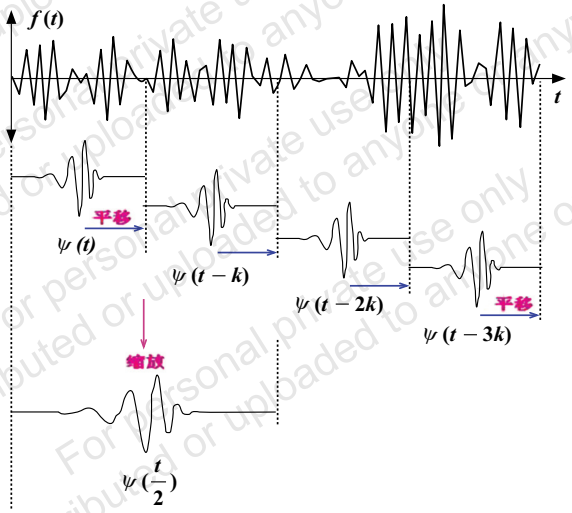

Fig. (1). Signal decomposition and extraction process of the wavelet transform signal. *(A higher resolution / colour version of this figure is available in the electronic copy of the article).*

Table 1. Correspondence between EEG signal analyses of scale and frequency.

Scale	5	6	7	8	9	10	11	12	13	14	15
Frequency (Hz)	52.02	34.68	23.12	15.41	10.28	6.85	4.58	3.04	2.03	1.35	0.90
Scale	16	17	18	19	20	21	22	23	24	25	26
Frequency (Hz)	0.60	0.40	0.27	0.18	0.12	0.08	0.05	0.04	0.02	0.02	0.01

2.3.2.2. Conditional Sampling - Phase Averaging

The average phase waveform of the EEG signal is regarded as the average wavelength of waveform activity in a certain frequency band. The unit of wavelength is time (s), and 1/s is the specific frequency of the wave in the corresponding frequency band, the unit for which is Hz [46].

The EEG signal $f(t,\alpha)$ was used as the detection condition, and the single wavelet coefficient at the α scale $W(t,\alpha)$ was detected. The maximum positive value was then calculated to obtain the average phase waveform. The calculation formula is as follows in Eq. (3):

$$D(t,\alpha)=\begin{cases}1, t\in\left[t_i-\frac{T(\alpha)}{2}, t_i+\frac{T(\alpha)}{2}\right]\\ 0, otherwise\end{cases} \quad (3)$$

The above sampling function formula is the corresponding conditional qualification; thus, it is also called the conditional sampling function. The original EEG signal $f(t)$ in Eq. (1) and the phase average waveform $D(t,\alpha)$ in Eq. (4) are multiplied to obtain $(t)D\cdot(t,\alpha)$. Therefore, unqualified signals are removed to leave only the qualified signals to enable conditional sampling of the original EEG signal. The screened EEG signal fragments were superimposed in terms of consistent length (wavelength and amplitude) and phase alignment, and phase averaging was subsequently performed to obtain the average phase waveform of the desired scale of each lead:

$$<f(t,\alpha)>=\frac{1}{N}\sum_{i=1}^{N} f\left(t+t_i-\frac{T(\alpha)}{2}\right)D(t_i,\alpha), t\in\left[-\frac{T(\alpha)}{2},\frac{T(\alpha)}{2}\right] \quad (4)$$

2.4. Statistical Analysis

All data were analyzed using the IBM SPSS Statistics 24 software (IBM SPSS Inc., Chicago, USA). Normally distributed data are expressed as means ± standard deviations, and non-normally distributed data are expressed as interquartile ranges. Clinical data and the average waveform wavelength of the ninth scale phase in different brain regions of the HC, mAD, and msAD groups were analyzed using analysis of variance for normally distributed data and the Kruskal-Wallis test for non-normally distributed data. If the Kruskal-Wallis test for the average waveform wavelength of the ninth scale phase in different brain regions showed a significant difference among the three groups, pairwise comparison between groups was performed by Mann-Whitney U test, and the results were corrected by Bonferroni. Spearman correlation analysis was used to investigate the correlation between the average waveform wavelength of the ninth-scale phase and the MMSE score. Receiver operating characteristic (ROC) curve analysis was used to evaluate the diagnostic accuracy of the α-rhythm wavelength of each lead, and the Youden Index was calculated to find the best cutoff value. The area under the ROC curve (AUC) was used to evaluate the diagnostic efficacy of the ninth scale phase average waveform wavelength in different leads. $P < 0.01$ indicated statistical significance. The Origin 2017 and GraphPad Prism 8.4.0 software were used for drawing the figures.

3. RESULTS

3.1. Clinical Data Analysis

The comparison results of clinical data among the three groups are shown in Table **2**. No significant differences in age, sex, or an educational level were found among the three groups ($P > 0.05$). The MMSE score differed significantly among the three groups ($P < 0.001$).

3.2. Original Visual EEG

Fig. (**2**) shows the original visual EEG of three subjects in the HC (a), mAD (b), and msAD (c) groups of the same sex and similar age, which is a typical representative of people with different cognitive levels. As shown in Fig. (**2a**), the visual background EEG of the HC was dominated by the α rhythm. There was a clear predominant α rhythm in the occipital region, which was mixed with a small amount of β and θ waves. As shown in Fig. (**2b**), the visual EEG showed that the α background rhythm was slower, the α rhythm was shifted forward, the dominance of the occipital region was less obvious, there were more θ waves in the background, and amplitude modulation was poorer in mAD patients than in HCs. Fig. (**2c**) shows that the background rhythm of the visual EEG of msAD patients was even slower than mAD patients, characterized by primarily the θ rhythm at approximately 5 Hz. There was almost no dominant α rhythm in the occipital region. Moreover, the waveform was irregular, and the amplitude modulation was poor. Henceforth, this rhythm change phenomenon is collectively referred to as the slowing of the α rhythm. Although the slowdown of this scale rhythm has exceeded the range of the α frequency band, the change of the average phase waveform of this scale is continuous in patients with different degrees of dementia, and it is still referred to as the slowdown of α rhythm in this paper.

3.3. Time-frequency Analysis of EEG Signals at Different Scales

The Gauss wavelet transform technique was used to decompose 20-seconds original EEG signals to study the time-frequency characteristics of EEG signals and understand the

Table 2. Demographic data.

Group	All Subjects	HC	mAD	msAD	$\chi 2/F/U$	*P*
Gender (F/M)	64/60	23/17	21/21	20/22	0.867	0.648
Age	71.09 ± 9.304	68.53 ± 9.543	73.31 ± 9.462	71.31 ± 8.487	2.807	0.064
Education	5.69 ± 2.173	6.18 ± 0.347	5.29 ± 0.341	5.62 ± 0.320	1.767	0.175
MMSE	22.00 (14.00,27.00)	29.00 (27.00,30.00)	22.00 (20.00,24.00)	10.50 (4.50,14.00)	109.396	<0.001

Fig. (2). Original visual EEG of HC (**a**; MMSE 30 points), mAD (**b**; MMSE 19 points), and msAD (**c**; MMSE 3 points) in a quiet state with eyes closed.

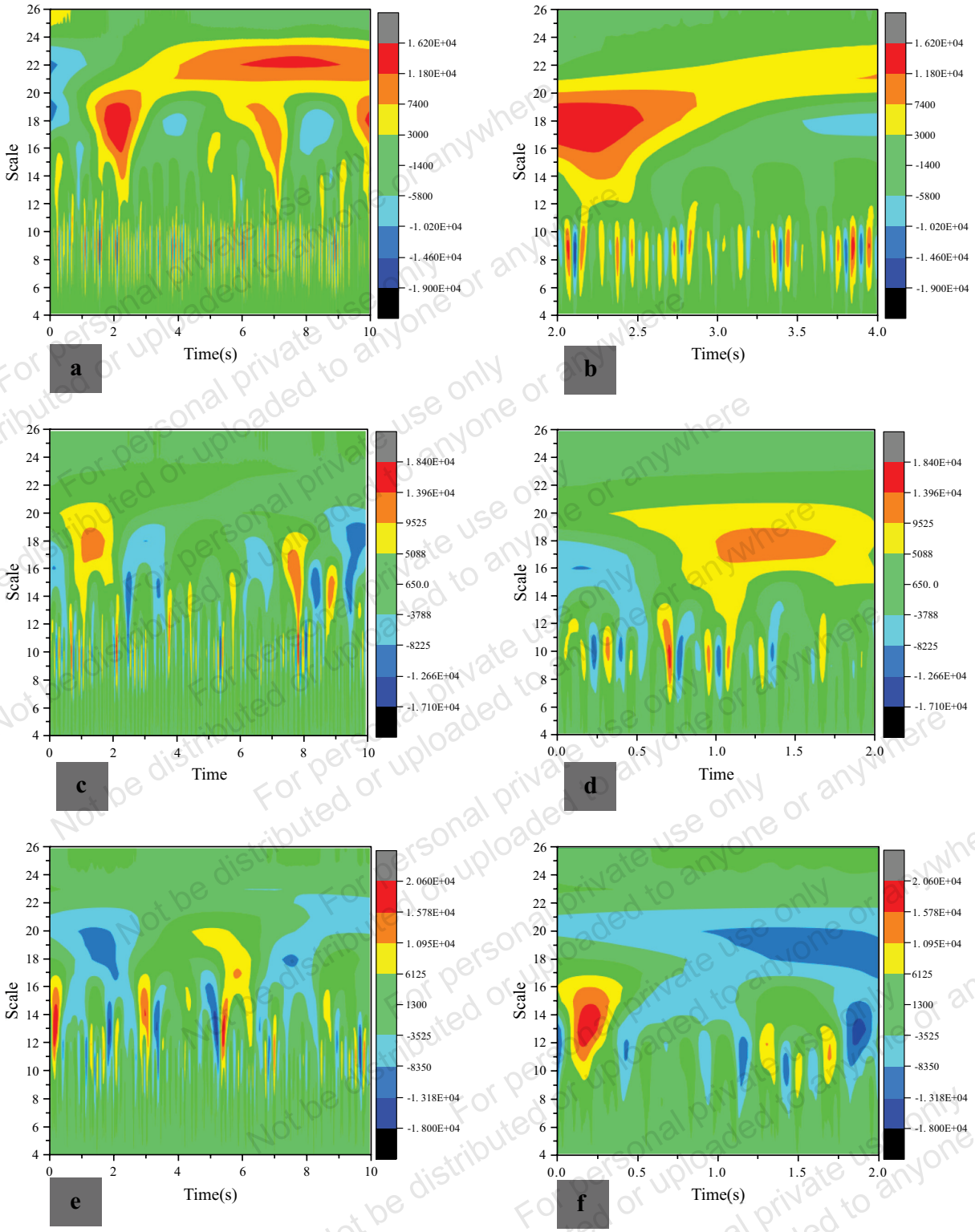

Fig. (3). Time-frequency analysis of EEG signals at different scales in HC (**a** and **b**; MMSE 30 points), mAD (**c** and **d**; MMSE 19 points), and msAD (**e** and **f**; MMSE 3 points). *(A higher resolution / colour version of this figure is available in the electronic copy of the article).*

relationship between different scales of EEG signals. Figs. (**3** and **3-f**) shows the time-frequency analysis diagrams of the EEG signals in the occipital region corresponding to Fig. (**2**) of the three subjects, respectively. The horizontal axis represents time (the sampling frequency was 200 Hz, corresponding to 1 s when converted into time), and the vertical axis represents the scale (the corresponding relationship with frequency is shown in Table **1**). The different colors indicate the amplitude (voltage) of the wavelet coefficient.

Figs. (**3a** and **b**) show the time-frequency structure characteristics of the EEG signals at different time resolutions (*i.e.,* 10 and 2 s, respectively) in HCs. The 10-s contour map shows an obvious "cascade coupling" relationship between different scales in HCs. The 21-scale structure generated a 17-scale envelope structure *via* bifurcation, and the 17-scale structure enveloped the nine-scale structure, which showed a clear hierarchical interconnecting relationship. The 2-s contour map shows rhythmic activity at the ninth scale below the 17-scale structure, which contained approximately 8-10 nine-scale structures per second.

Figs. (**3c** and **d**) show the time-frequency structure characteristics of the EEG signals in mAD patients at different time resolutions (*i.e.,* 10 and 2 s, respectively). The 10-second contour map shows that the "cascade coupling" relationship between different scales was disordered, and the scale structure was not rich. The 2-s contour map shows rhythmic activity at the 10th scale below the 17-scale structure, and there were approximately 6-8 10-scale structures per second, corresponding to a frequency of approximately 6 Hz. These results indicated that the α band of mAD patients moved to a higher scale than that of HCs; that is, the α rhythm slowed down.

Figs. (**3e** and **f**) shows the time-frequency structure characteristics of EEG signals in msAD patients at different time resolutions (*i.e.,* 10 and 2 s, respectively). The comparison of contour plots among subjects a, b and c showed that as AD progressed, the scale structure became simplified, and the "cascade coupling" structure gradually deteriorated and was destroyed. The α band of msAD patients moved to a higher scale, approaching the 11th scale, and the slowing of the α rhythm was more evident in these patients than in HCs and mAD patients.

3.4. EEG Waveform Activity of the Ninth Scale

We examined the waveform activity characteristics of the ninth scale in the occipital region corresponding to the α frequency band. Fig. (**4**) shows the activity waveforms of the main rhythm in the occipital region of the above three subjects. The 10- and 2-s data with stable signals are shown in the figure. The 10-s α-wave shape characteristics of the HC (Fig. **4a**)**,** MMSE 30 points), mAD (Fig. **4c**)**,** MMSE 19 points), and msAD subjects (Fig. **4e**)**,** MMSE 3 points) showed that the α-wave density decreased significantly as cognitive function declined. The 2-s pattern of the three subjects showed that the occipital region of HCs (Fig. **4b**) was dominated by an α rhythm of 9-10 Hz, and the amplitude modulation was good. In mAD (Fig. **4d**) patients, the background occipital α rhythm was slow at approximately 7-8 Hz, and the amplitude modulation was poor. The EEG of the msAD (Fig. **4f**) patients showed that the background rhythm was even slower at approximately 5-6 Hz.

3.5. Phase Average Waveform Analysis of the EEG Signal of the Ninth Scale

We extracted the phase average waveform characteristics of the ninth scale in different leads, which were the frequency bands of the visual EEG of healthy awake adults in a quiet state with eyes closed. The corresponding center frequency was 10 Hz. Fig. (**5**) represent the phase average waveform characteristics of lead O1 of the ninth scale in the three subjects, respectively, corresponding to Fig. (**2**). The average waveform wavelength of the ninth-scale phase in the lead of HC was approximately 0.1 s, and the corresponding center frequency was 10 Hz, corresponding to the α frequency band. The average waveform wavelength of the lead in mAD subject was approximately 0.13 s, and the corresponding center frequency was 7-8 Hz. The average waveform wavelength of the ninth-scale phase in the lead of msAD subject was approximately 0.16 s, which corresponded to a center frequency of 6.25 Hz. The comparison of the average phase waveforms among the three subjects with different wavelengths revealed that the average waveform wavelength of the ninth scale gradually lengthened as the cognitive function of patients declined, and the α frequency gradually slowed. Thus, the slow α frequency of the EEG signal gradually slowed with the progression of AD. We found that the average waveform wavelength of the ninth-scale phase was highest in msAD patients, followed by mAD patients and HCs.

The Kruskal-Wallis test was used to compare the average wavelength of the ninth-scale phase of EEG signals in different brain regions (16 leads) among mAD patients, msAD patients, and HCs. As shown in Table **3**, results showed significant differences in the wavelength of the average waveform of the ninth-scale phase of EEG signals among the three groups under a spontaneous state. In the HC and mAD groups, the wavelengths of the parietal and occipital regions were shorter than those of the anterior head and temporal regions, which is consistent with the dominant rhythm distribution characteristics of the occipital region. However, in msAD patients, the wavelengths of each lead across the brain were similar, and there were no obvious dominant rhythm distribution characteristics. The wavelength of msAD patients was greater than that of the mAD patients and HC subjects. The results of the pairwise comparisons by the Mann-Whitney U test between the groups are shown in Table **4**. Except for the T6 lead of mAD and msAD patients, the average wavelength of the ninth-scale phase of the leads differed significantly between groups ($P < 0.01$). To more directly observe the average waveform wavelength characteristics of the ninth-scale phase of different leads in the three groups, we drew a violin plot (Fig. **6**), which showed that as cognitive function declined, the wavelength increased, and the EEG signal slowed. Furthermore, the wavelength of several msAD patients was greater than 0.2 s, which is equivalent to a scale-corresponding frequency of over 5 Hz, approaching or reaching the θ band.

3.6. Correlation Analysis between the Phase Average Waveform Wavelength of the Ninth Scale and the MMSE Score

To examine the relationship between the average waveform wavelength of the ninth scale and the severity of AD, we performed a correlation analysis between the phase average waveform wavelength at the ninth scale in different leads and the MMSE score. Fig. (**7**) shows a scatter plot of the correlation in different leads. In all leads, we found that as the MMSE score decreased, the phase average waveform wavelength of the ninth scale became larger, as evidenced by a significant negative correlation. The Spearman correlation analysis results showed all leads were significant (Table **5**),

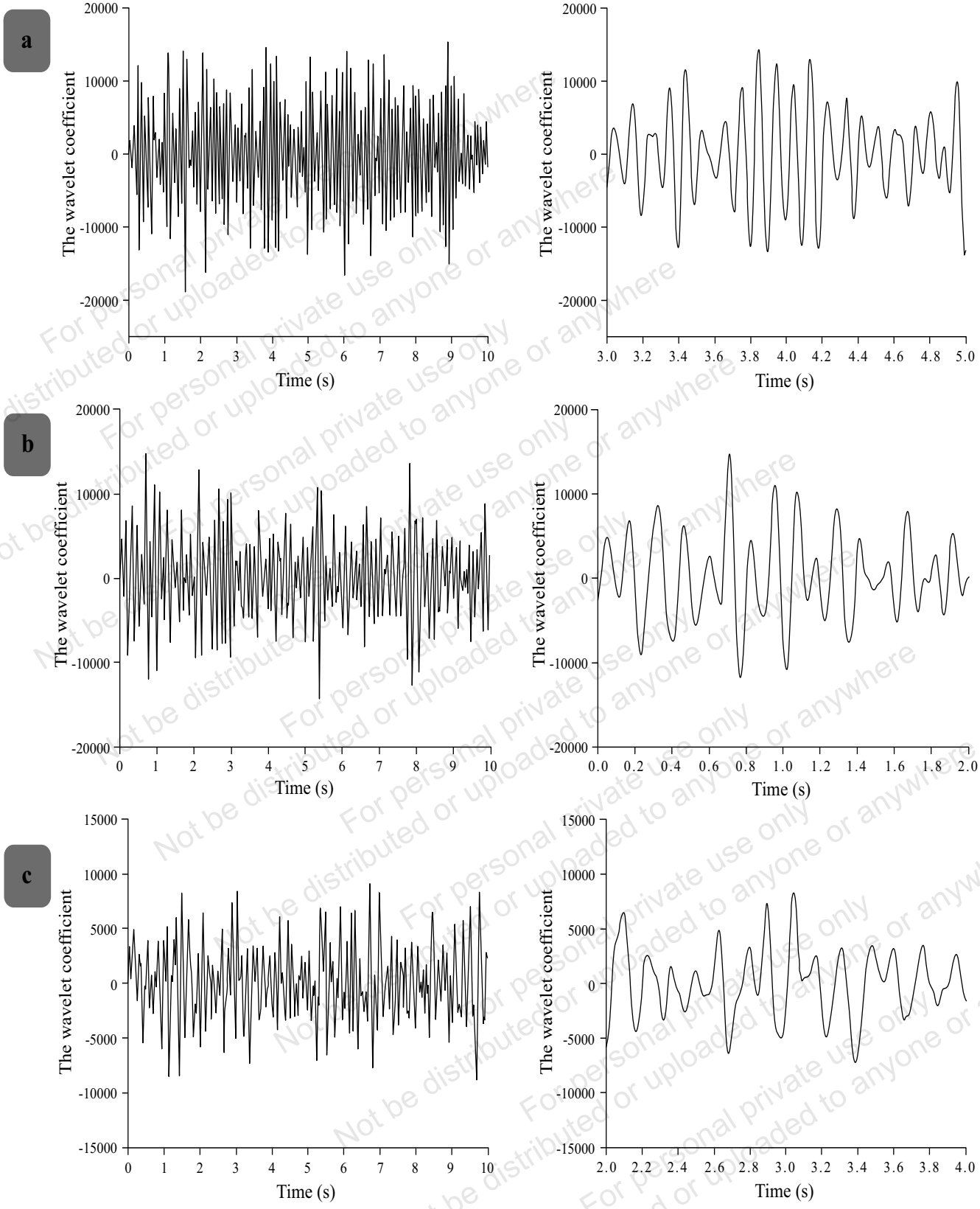

Fig. (4). Waveform activity of EEG signals in the occipital region of an HC (**a** and **b**; MMSE 30 points), an mAD (**c** and **d**; MMSE 19 points), and an msAD subject (**e** and **f**; MMSE 3 points) at the ninth scale for 10 s and 2 s. *(A higher resolution / colour version of this figure is available in the electronic copy of the article).*

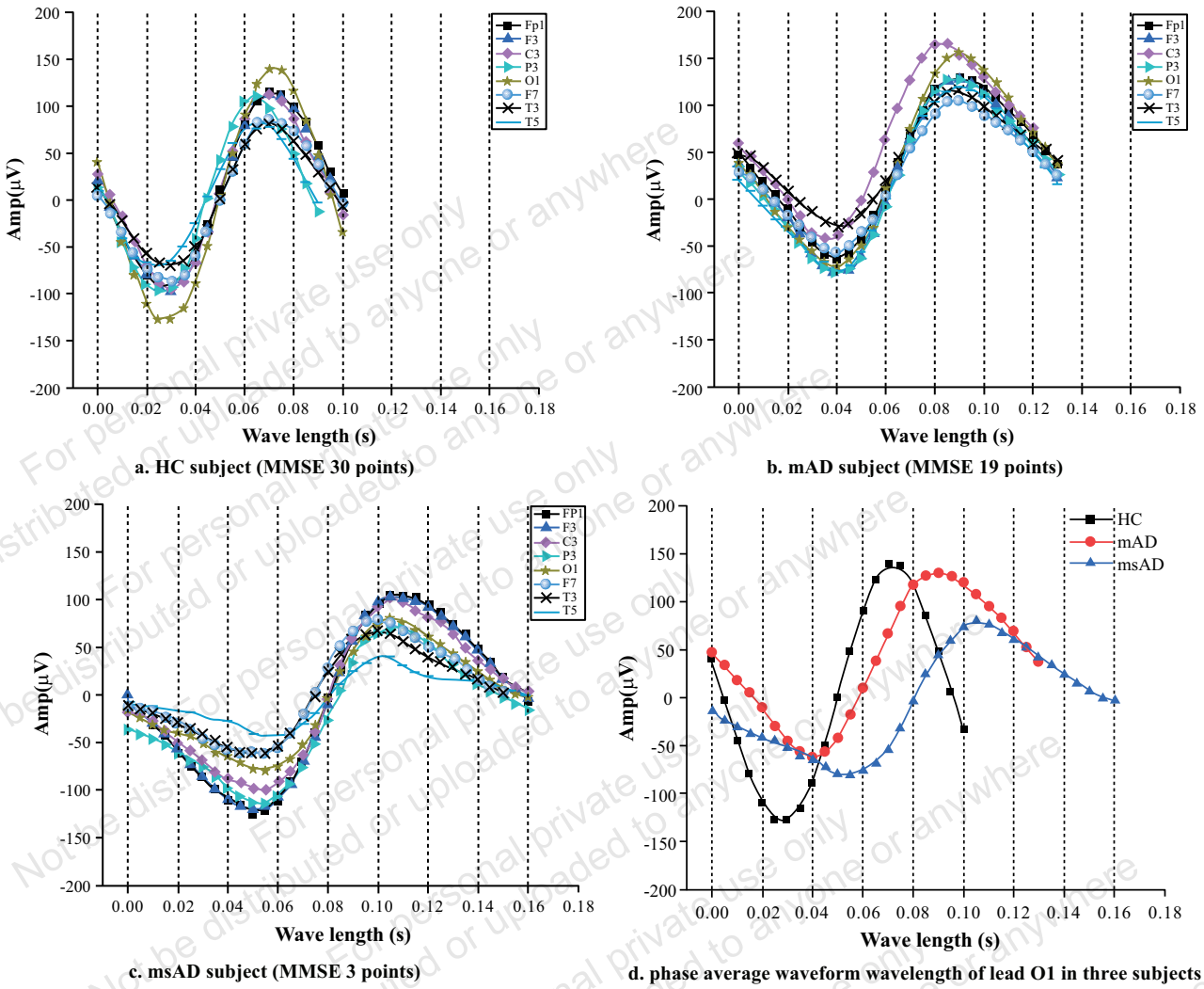

Fig. (5). (**a-c**), respectively, show the ninth-scale phase average waveform characteristics of different brain regions in the left hemisphere of HC, mAD, and msAD subjects. (**d**) shows the average waveform wavelength of the ninth scale of lead O1 in HC, mAD, and msAD subjects. *(A higher resolution / colour version of this figure is available in the electronic copy of the article).*

and the strongest correlation was found in lead P3 (ρ = 0.721, $P < 0.001$). There were no significant correlations between the phase average waveform wavelength of the ninth scale and age, sex, or educational level ($P > 0.05$).

3.7. ROC Curve Analysis

The ROC curve analysis was performed on the phase average waveform wavelength of the ninth scale between HCs and mAD patients, HCs and msAD patients, mAD and msAD patients, and HCs and all AD patients. The results are shown in (Fig. **8** and Table **6**). For the comparison between the HCs and the mAD patients, the diagnostic efficacy of the phase average waveform wavelength of the ninth scale of all leads except T4 was higher than 70%. The AUC of lead P3 was the largest (AUC = 0.805, $P < 0.001$), which indicated that this lead had the greatest diagnostic efficacy. For the comparison between HCs and msAD patients, the diagnostic efficiency of the phase average waveform wavelength of the ninth scale in all leads was higher than 80%, and the AUC of lead P3 was the largest (AUC = 0.940, $P < 0.001$), indicating that this lead had the greatest diagnostic efficiency. For the comparison between the mAD and msAD patients, the diagnostic efficiency of the phase average waveform wavelength of the ninth scale in all leads was higher than 70%, and the FP1 lead had the largest AUC (AUC = 0.812, $P < 0.001$) and thus had the greatest diagnostic efficiency. For the comparison between HCs and all AD patients, the diagnostic efficiency of the phase average waveform wavelength of the ninth scale in all leads was higher than 70%, and the AUC of lead P3 was the largest (AUC = 0.873, $P < 0.001$), which indicated that this lead had the greatest diagnostic efficacy.

The wavelength of the average phase waveform of the ninth scale showed a higher correct index for the diagnosis of AD patients. As shown in Table **7**, among the 16 leads across the brain, the Youden Index of the phase average waveform wavelength of the ninth scale in lead P3 reached 0.668, with a sensitivity of 89.3% and a specificity of 77.5%. A phase average waveform wavelength of the ninth scale of lead P3 of 0.11 seconds was determined to be the critical value for differentiating AD patients from HCs.

Table 3. Comparison results of the phase average waveform wavelength of the ninth scale of subjects in the HC, mAD, and msAD groups.

Lead	HC	The Median (P25, P75)	msAD	U	*P*
		mAD			
	(n=40)	(n=42)	(n=42)		
FP1	0.110 (0.103, 0.119)	0.120 (0.116, 0.130)	0.140 (0.130, 0.160)	57.319	<0.001
FP2	0.110 (0.103, 0.120)	0.120 (0.115, 0.130)	0.140 (0.128, 0.153)	47.134	<0.001
F3	0.110 (0.100, 0.112)	0.120 (0.110, 0.130)	0.130 (0.127,0.160)	55.358	<0.001
F4	0.110 (0.100, 0.118)	0.120 (0.110, 0.129)	0.131 (0.128, 0.160)	53.448	<0.001
C3	0.105 (0.100, 0.110)	0.120 (0.110, 0.122)	0.130 (0.120, 0.150)	59.564	<0.001
C4	0.105 (0.100, 0.116)	0.112 (0.110, 0.121)	0.130 (0.120, 0.160)	47.838	<0.001
P3	0.100 (0.098, 0.110)	0.113 (0.110,0.125)	0.135 (0.120, 0.150)	60.449	<0.001
P4	0.104 (0.100, 0.110)	0.110 (0.110, 0.129)	0.130 (0.120, 0.150)	42.549	<0.001
O1	0.102 (0.100, 0.110)	0.110 (0.110, 0.120)	0.140 (0.120, 0.150)	58.359	<0.001
O2	0.102 (0.100, 0.110)	0.110 (0.110, 0.120)	0.130 (0.120, 0.150)	49.716	<0.001
F7	0.110 (0.102, 0.112)	0.120 (0.110, 0.130)	0.140 (0.130, 0.150)	54.083	<0.001
F8	0.110 (0.102, 0.118)	0.120 (0.110, 0.130)	0.140 (0.120, 0.143)	41.420	<0.001
T3	0.102 (0.100, 0.110)	0.113 (0.110, 0.123)	0.140 (0.120, 0.150)	58.720	<0.001
T4	0.110 (0.100, 0.119)	0.117 (0.110, 0.130)	0.130 (0.110, 0.150)	29.127	<0.001
T5	0.105 (0.100,0.110)	0.120 (0.110, 0.126)	0.135 (0.120, 0.150)	55.631	<0.001
T6	0.110 (0.100, 0.116)	0.120 (0.110, 0.130)	0.130 (0.118, 0.143)	30.054	<0.001

Table 4. Comparison and statistical analysis results of the phase average waveform wavelength of subjects in the HC, mAD, and msAD groups.

-	HC VS mAD	HC VS msAD	mAD VS msAD
	Z (*P*)	*Z* (*P*)	*Z* (*P*)
FP1	-3.551 (0.001)	-7.562 (<0.001)	-4.060 (<0.001)
FP2	-3.553 (0.001)	-6.865 (<0.001)	-3.354 (0.002)
F3	-3.735 (0.001)	-7.440 (<0.001)	-3.751 (0.001)
F4	-3.476 (0.002)	-7.304 (<0.001)	-3.876 (<0.001)
C3	-3.857 (<0.001)	-7.717 (<0.001)	-3.908 (<0.001)
C4	-3.039 (0.007)	-6.893 (<0.001)	-3.902 (<0.001)
P3	-3.941 (<0.001)	-7.775 (<0.001)	-3.881 (<0.001)
P4	-3.108 (0.006)	-6.517 (<0.001)	-3.452 (0.002)
O1	-3.645 (0.001)	-7.633 (<0.001)	-4.037 (<0.001)
O2	-3.084 (0.006)	-7.025 (<0.001)	-3.991 (<0.001)
F7	-3.508 (0.001)	-7.348 (<0.001)	-3.888 (<0.001)
F8	-3.221 (0.004)	-6.435 (<0.001)	-3.255 (0.003)
T3	-3.789 (<0.001)	-7.661 (<0.001)	-3.920 (<0.001)
T4	-2.421 (0.046)	-5.383 (<0.001)	-2.998 (0.008)
T5	-3.606 (0.001)	-7.454 (<0.001)	-3.896 (<0.001)
T6	-3.336 (0.003)	-5.445 (<0.001)	-2.135 (0.098)

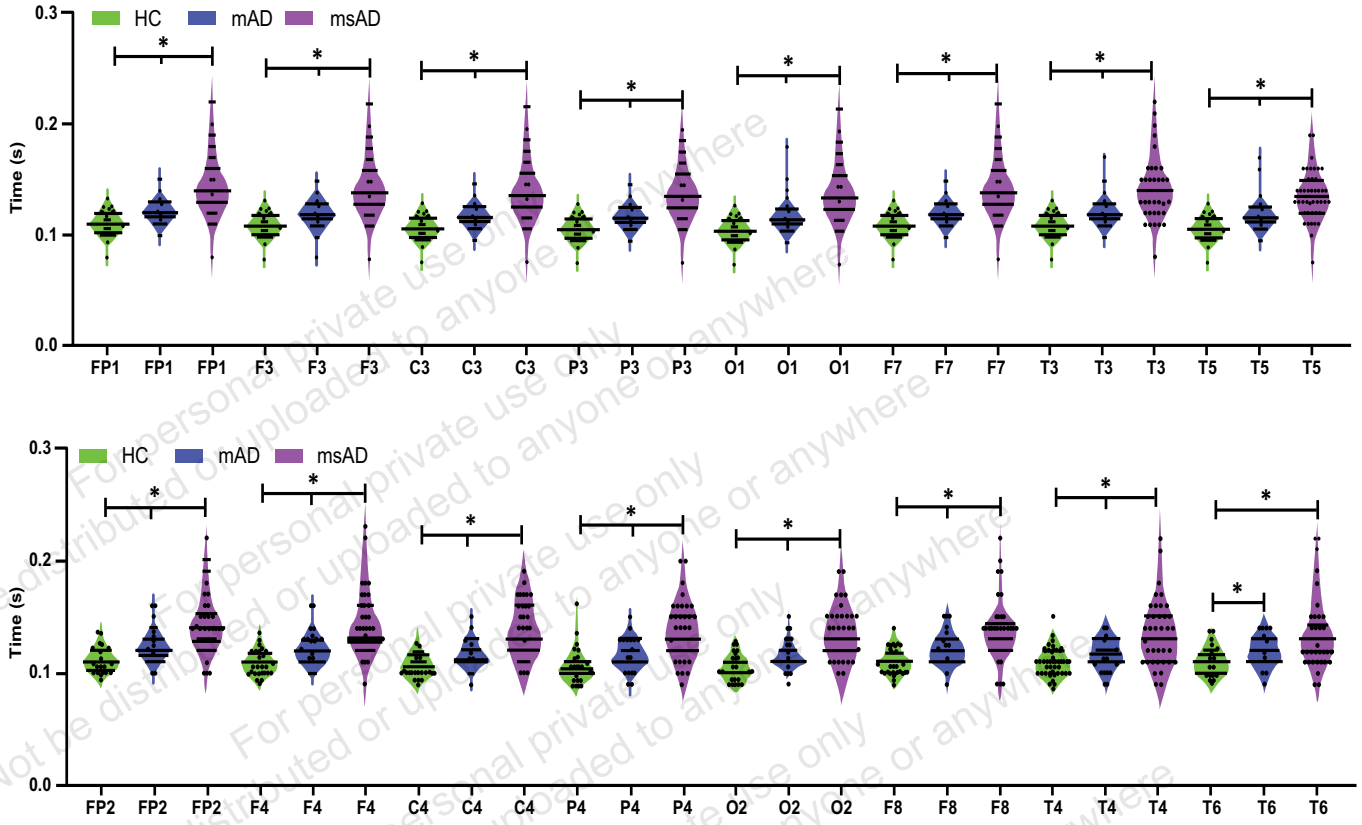

Fig. (6). Comparison of the phase average waveform wavelength of the ninth scale EEG signal in different leads between the AD patients and HCs. *(A higher resolution / colour version of this figure is available in the electronic copy of the article).*

4. DISCUSSION

According to traditional visual EEG analysis, as cognitive function declines, dementia patients may exhibit various visual EEG features, such as slowing of background rhythm frequency and adjustment and amplitude modulation changes; however, it is difficult to distinguish early AD patients [25]. Therefore, extracting accurate waveform features to identify early disease states is crucial. Our aim was to identify simple EEG biomarkers that respond during rest state. We decomposed EEG signals at different scales using wavelet transform analyses and determined EEG characteristics in terms of time and frequency simultaneously. The phase averaging technique enables the extraction of multi-scale phase-averaging waveforms from EEG signals. The main advantage of this technique is its ability to detect the components of EEG signals with similar rhythms by establishing basic rhythmic activity characteristics of different scale components of EEG signals, intercepting the original complex non-linear EEG signals into segments with the same components, superimposing these in phase alignment, and conducting phase alignment averaging to obtain the average waveform characteristics of EEG signals at certain scales and time periods. This enabled us to confirm that the phase average waveform wavelength reflects the frequency characteristics of EEG signals.

We extracted the average, typical waveform features of the ninth-scale phase of the background rhythm of EEG signals as an index of α-rhythm characteristics that corresponded to a center frequency of approximately 10 Hz. We found a significant difference in the phase average waveform wavelength of the ninth scale (*i.e.,* the average wavelength of the α rhythm phase) between AD patients and HCs. We revealed that the wavelength of the phase average waveform of the α rhythm in HCs was within 0.11 s, which corresponded to an α-rhythm frequency of roughly 9 Hz. The wavelength of the phase average waveform in AD patients was between 0.11 and 0.16 s, which scale corresponded to the frequency of approximately 6-9 Hz. Moreover, the wavelength of several patients with severe dementia reached as high as 0.20 s, which scale corresponded to the frequency of approximately 5 Hz. A normal α rhythm involves the synchronization of a large number of neurons and ensures a normal transmission speed of cognitive information between cortical neurons with the same phase and frequency oscillation; this allows the cortical network to process cognitive information at an appropriate speed [47]. The slow rhythm of the α-phase average waveform in patients with AD may be related to the loss of cholinergic neurons projecting to the hippocampus and neocortex [21], and the synchronous activity of neurons involved in cognition, which slows information transmission, reduces the ability to further process and integrate information, eventually leading to brain atrophy and cognitive dysfunction [19]. Studies have shown that the MMSE score of AD patients is negatively correlated with the wavelength

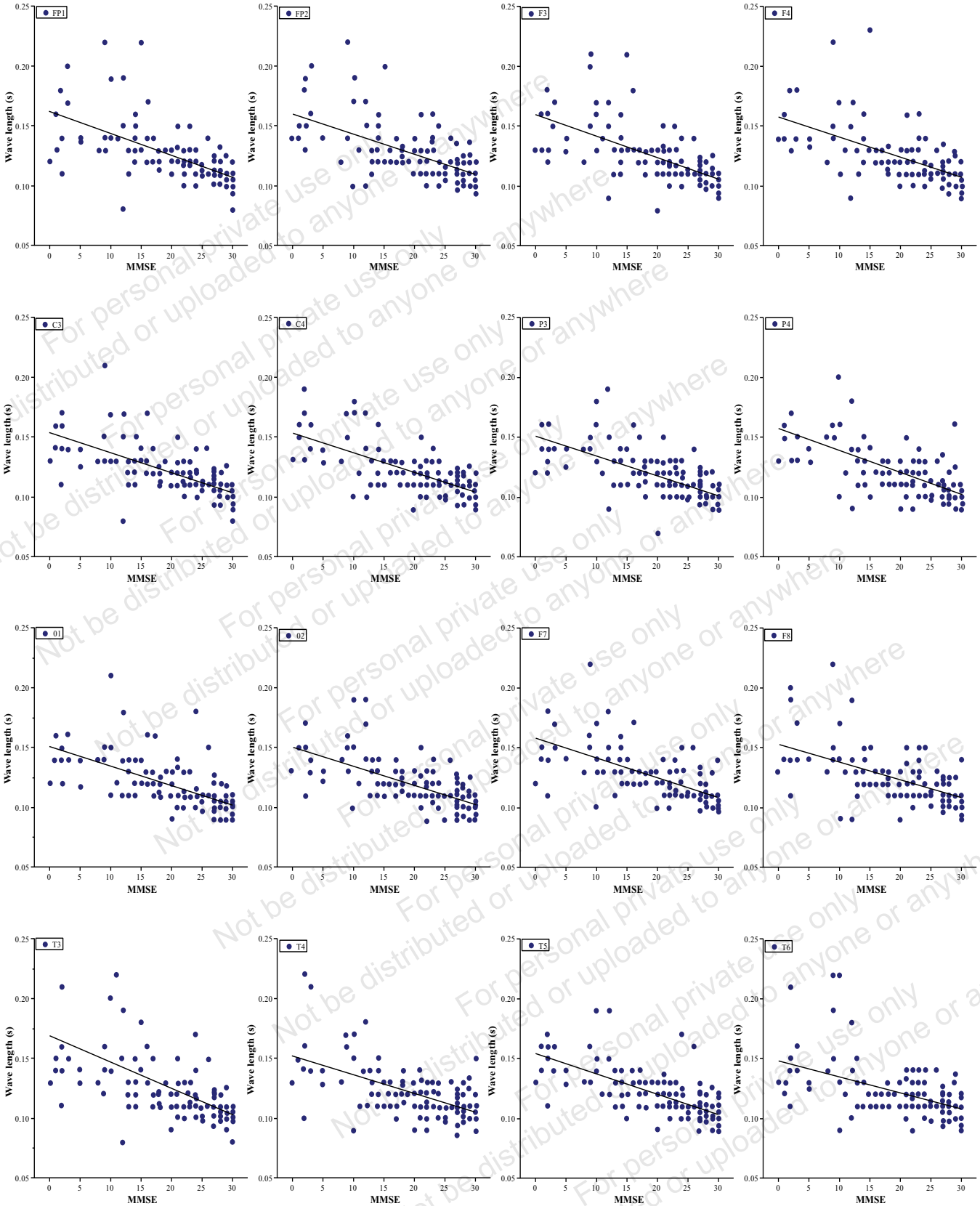

Fig. (7). Scatter plot of the relationship between the phase average waveform wavelength of the ninth scale and MMSE score in different brain regions of all subjects. *(A higher resolution / colour version of this figure is available in the electronic copy of the article).*

Table 5. Correlation between the phase average waveform wavelength of the ninth scale and MMSE score in all subjects.

Lead	FP1	F3	C3	P3	O1	F7	T3	T5
ρ	-0.689	-0.687	-0.718	-0.721	-0.709	-0.666	-0.701	-0.702
P	<0.001	<0.001	<0.001	<0.001	<0.001	<0.001	<0.001	<0.001
Lead	**FP2**	**F4**	**C4**	**P4**	**O2**	**F8**	**T4**	**T6**
ρ	-0.644	-0.669	-0.651	-0.619	-0.673	-0.595	-0.534	-0.521
P	<0.001	<0.001	<0.001	<0.001	<0.001	<0.001	<0.001	<0.001

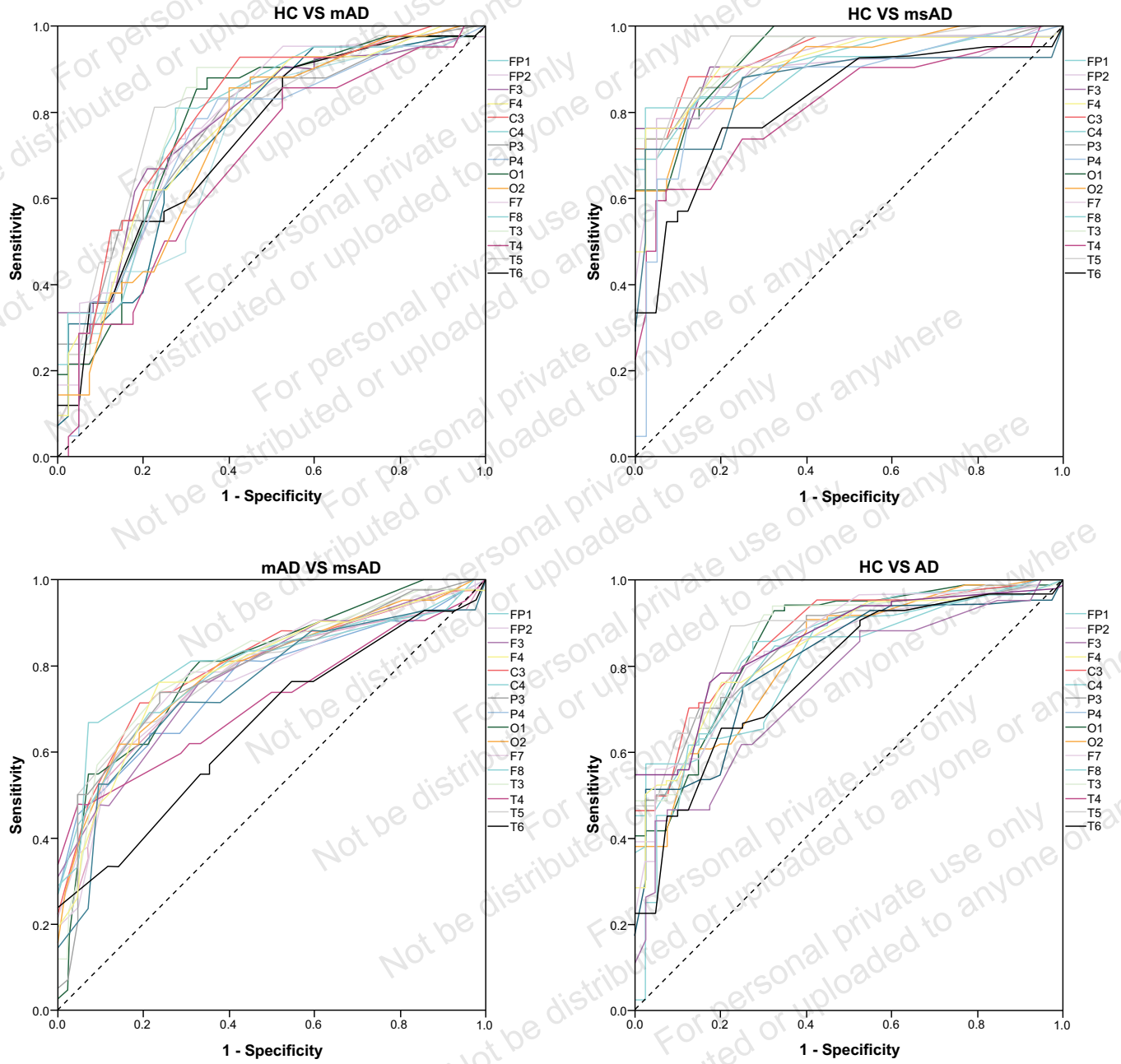

Fig. (8). ROC curves of the phase average waveform wavelength of the ninth scale of each lead in different groups. *(A higher resolution / colour version of this figure is available in the electronic copy of the article).*

Table 6. Area and significance under the ROC curve of the phase average waveform wavelength of the ninth scale of each lead.

Lead	HC VS mAD		HC VS msAD		mAD VS msAD		HC VS AD	
	AUC	*P*	AUC	*P*	AUC	*P*	AUC	*P*
FP1	0.786	<0.001	0.921	<0.001	0.812	<0.001	0.853	<0.001
FP2	0.773	<0.001	0.889	<0.001	0.756	<0.001	0.831	<0.001
F3	0.783	<0.001	0.927	<0.001	0.779	<0.001	0.855	<0.001
F4	0.767	<0.001	0.918	<0.001	0.787	<0.001	0.842	<0.001
C3	0.803	<0.001	0.932	<0.001	0.801	<0.001	0.868	<0.001
C4	0.733	<0.001	0.898	<0.001	0.783	<0.001	0.815	<0.001
P3	0.805	<0.001	0.940	<0.001	0.796	<0.001	0.873	<0.001
P4	0.744	<0.001	0.868	<0.001	0.761	<0.001	0.806	<0.001
O1	0.778	<0.001	0.935	<0.001	0.798	<0.001	0.856	<0.001
O2	0.736	<0.001	0.905	<0.001	0.789	<0.001	0.821	<0.001
F7	0.773	<0.001	0.916	<0.001	0.792	<0.001	0.845	<0.001
F8	0.748	<0.001	0.865	<0.001	0.746	<0.001	0.807	<0.001
T3	0.795	<0.001	0.933	<0.001	0.798	<0.001	0.864	<0.001
T4	0.683	0.004	0.813	<0.001	0.716	0.001	0.748	<0.001
T5	0.772	<0.001	0.932	<0.001	0.785	<0.001	0.852	<0.001
T6	0.737	<0.001	0.820	<0.001	0.658	0.013	0.779	<0.001

Table 7. Sensitivity, specificity, Youden index, and cutoff score of the ROC curve analysis of the phase average waveform wavelength of the ninth scale of 16 leads in AD and HC subjects.

Lead	Sensitivity (%)	Specificity (%)	Youden Index	Cut off
FP1	85.7	72.5	0.582	0.113281
FP2	82.1	72.5	0.546	0.118828
F3	76.2	82.5	0.587	0.118594
F4	76.2	80.0	0.562	0.118830
C3	70.2	87.5	0.577	0.118595
C4	63.1	85.0	0.481	0.118830
P3	89.3	77.5	0.668	0.109920
P4	84.5	67.5	0.520	0.109922
O1	92.9	67.5	0.604	0.109690
O2	90.5	60.0	0.505	0.107423
F7	77.4	77.5	0.549	0.113281
F8	75.0	75.0	0.500	0.111641
T3	91.7	70.0	0.617	0.109690
T4	44.0	95.0	0.390	0.129455
T5	70.2	85.0	0.552	0.119922
T6	65.5	80.0	0.455	0.119922

of the average phase waveform, where the phase average waveform wavelength of the ninth scale in AD patients increases gradually as dementia progresses, and the frequency is slower. In AD patients, the α rhythm slows, the degree to which can reach the θ or δ frequency band; this is known as α-rhythm slowing down. Our results showed that the average α-rhythm phase waveforms in all leads differed significantly among the HC, mAD, and msAD groups. Thus, we suggest that the slowing of α-rhythm frequency is an important biomarker for differentiating AD patients from HCs.

Although the slowing of the α rhythm has been demonstrated in numerous studies, most previous studies only studied EEG slowing in dementia patients regarding power or amplitude [35, 48]. In contrast, we calculated the wavelength of the background rhythm of different individuals in the rest state to examine the α-rhythm frequency. We found that the more severe the dementia, the slower the EEG activity, and the longer the wavelength of the background rhythm, the lower the α frequency. Moreover, even the θ band rhythm can be reached in severe cases, although this is not the real meaning of the θ rhythm, but rather a slowing phenomenon of the α rhythm. This finding is consistent with previous studies investigating power, where α frequency and power change are non-linearly correlated [47]. Several studies have demonstrated that the background rhythm of EEG slows during the normal aging process in healthy older adults. Compared with middle-aged adults aged 30-50 years, the α frequency of older adults aged 60-80 years is approximately 1 Hz slower, characterized as a decrease in α amplitude in the posterior brain region, which may be related to the decline in cholinergic neuronal function in the basal ganglia [6]. Studies have also speculated that the slowing is not caused by aging but by age-related neurological diseases [47]. We also found that the average α-rhythm frequency of the older adult HCs was approximately 9 Hz, which is lower than the standard frequency of a younger healthy adult average (approximately 10 Hz). However, we did not find a correlation between the average waveform wavelength of the α phase and age change. This may be because there was little variation in the age of the subjects in our study, where the average age was approximately 70 years. The brain wave shape of each group is relatively stable at this age stage, and the benign changes affected by age do not differ in individuals of this age group. To identify the factors that influence EEG changes during the process of normal aging, future studies should compare patients with age-matched healthy older adults to exclude the confounding factor of age.

In 1999, Klimesch proposed that frequency and power are closely related metrics. The process of extracting individual alpha frequency (IAF) involves the calculation of the power spectrum distribution of individual EEG signals. The second power peak (*i.e.,* the lower power peak) was selected as the α-frequency band and defined as the IAF value, and the frequency range of low- and high-frequency α was delineated around the peak [47]. Babiloni *et al.* [35] used the same method to delineate the α-frequency range in people with different levels of cognitive function. However, this algorithm is limited to determining the α frequency according to the location of the peak power, and its main purpose is to provide the range of EEG band division in a study population. Moreover, the accuracy is poor, and it does not reflect individuals' average frequency of the real α rhythm. Therefore, a more effective and accurate index is needed to quantify the slowing of the α rhythm. Our results showed that the phase average waveform wavelength avoids the interference of other scale information and only reflects the essence of the information of the α-rhythm.

Babiloni *et al.* found that the occipital α rhythm amplitude can classify HC and AD subjects effectively, with a sensitivity of 87.8%, a specificity of 66.7%, and an AUC of 0.81 [35]. In addition, Cassani *et al.* achieved 91% accuracy in classifying HCs and AD patients using α spectral power and coherence. However, despite the high classification accuracy, they did not correct for age, sex, or educational level [5]. Ozbek *et al.* found that a decrease in α/θ power ratio was the best index for differentiating early-onset AD patients from young HCs, with sensitivity and specificity of over 80% and an AUC of 0.881. They suggested that patients with early-onset AD may have more extensive electrophysiological abnormalities than those with late-onset AD [6]. Collectively, previous studies have achieved classification accuracies of approximately 80% using EEG spectrum markers to differentiate AD patients from HCs [49]. We showed that the average phase waveform of the α rhythm in various brain regions differed significantly among HCs, mAD patients, and msAD patients, and the parietal region showed the largest difference. Moreover, we achieved a sensitivity of 89.3%, a specificity of 77.5%, and an AUC was 0.873, which were more significant than power and amplitude. A phase average waveform wavelength of the α rhythm in lead P3 of 0.11 s was the optimal cut-off value to distinguish AD from HCs. The normal human α rhythm is dominant in the occipital region of the visuospatial cortex [50]. We found that the phase average waveform wavelength of the ninth scale in lead P3 was most strongly correlated with the MMSE score, and the diagnostic efficiency of distinguishing HCs from AD patients was the greatest in this lead. We speculate that this may be related to the shifting forward of the α rhythm and the disappearance of a dominant rhythm in the occipital region in dementia patients [47]. Cicalese *et al.* similarly found that the left parietal lobe is closely related to AD-related cognitive decline using machine learning combined with EEG and functional near-infrared spectroscopy [51]. Previous studies have suggested that the precuneus in the parietal lobe and the posterior cingulate cortex are landmark regions of brain damage in AD patients, as evidenced by the deposition of pathological material and reduction in gray matter volume. As AD progresses, the parietal network becomes disrupted, and functional connectivity is reduced [19, 52] , which may explain why the slowing of the α rhythm is more prominent in the parietal lobe.

Our study had several limitations. Because of the severity of cognitive impairment in some AD patients, the EEG data of subjects in the dementia group were not normally distributed. In the future, we plan to increase the sample size, expand the study population, and include patients with mild cognitive impairment to further verify the sensitivity, specificity, and accuracy of the phase average waveform as a diagnostic biomarker for AD.

CONCLUSION

Our study aimed to identify simple EEG biomarkers for the diagnosis of AD. Our findings suggest that the phase average waveform wavelength of the ninth scale can be used as an electrophysiological biological marker for AD diagnosis with high accuracy and may serve as a simple auxiliary diagnostic tool for early screening of AD on a large scale and a non-invasive biomarker of neurodegeneration.

LIST OF ABBREVIATIONS

AD	=	Alzheimer's Disease
EEG	=	Electroencephalography
Aβ	=	β-amyloid
CSF	=	Cerebrospinal Fluid
p-TAU 181	=	Phosphorylated Tau Protein
MRI	=	Magnetic Resonance Imaging
HC	=	Healthy Controls
mAD	=	Mild AD
msAD	=	Moderately Severe AD
ADL	=	Abilities of Daily Living Scale
CDR	=	Clinical Dementia Rating Scale
MMSE	=	Mini-mental State Examination
CWT	=	Continuous Wavelet Transform
ROC	=	Receiver Operating Characteristic
AUC	=	Area Under the ROC Curve
IAF	=	Individual Alpha Frequency

ETHICS APPROVAL AND CONSENT TO PARTICIPATE

Approval of this study was obtained from the Ethics Committee of Tianjin Union Medical Center (Approval no.: 2022-B38).

HUMAN AND ANIMAL RIGHTS

No animals were used in this study. All human procedures were followed in accordance with the World Medical Association (Declaration of Helsinki) and the standards established by the Institutional Review Board.

CONSENT FOR PUBLICATION

Patient consent were obtained.

AVAILABILITY OF DATA AND MATERIALS

Not applicable.

FUNDING

This study was supported by the Project of Tianjin Union Medical Center (Grant No. 2018YJ020) and Major Diseases Special Project of Tianjin Science and Technology Commission (Grant No. 18ZXDBSY00120).

CONFLICT OF INTEREST

The authors declare no conflict of interest, financial or otherwise.

ACKNOWLEDGEMENTS

Declared none.

REFERENCES

[1] Knopman DS, Amieva H, Petersen RC, *et al.* Alzheimer disease. Nat Rev Dis Primers 2021; 7(1): 33. http://dx.doi.org/10.1038/s41572-021-00269-y PMID: 33986301

[2] Miao Y, Jurica P, Struzik ZR, *et al.* Dynamic theta/beta ratio of clinical EEG in Alzheimer's disease. J Neurosci Methods 2021; 359: 109219. http://dx.doi.org/10.1016/j.jneumeth.2021.109219 PMID: 34029602

[3] Tülay EE, Güntekin B, Yener G, Bayram A, Başar-Eroğlu C, Demiralp T. Evoked and induced EEG oscillations to visual targets reveal a differential pattern of change along the spectrum of cognitive decline in Alzheimer's Disease. Int J Psychophysiol 2020; 155: 41-8. http://dx.doi.org/10.1016/j.ijpsycho.2020.06.001 PMID: 32522511

[4] Farina FR, Emek-Savaş DD, Rueda-Delgado L, *et al.* A comparison of resting state EEG and structural MRI for classifying Alzheimer's disease and mild cognitive impairment. Neuroimage 2020; 215: 116795. http://dx.doi.org/10.1016/j.neuroimage.2020.116795 PMID: 32278090

[5] Cassani R, Falk TH, Fraga FJ, Cecchi M, Moore DK, Anghinah R. Towards automated electroencephalography-based Alzheimer's disease diagnosis using portable low-density devices. Biomed Signal Process Control 2017; 33: 261-71. http://dx.doi.org/10.1016/j.bspc.2016.12.009

[6] Özbek Y, Fide E, Yener GG. Resting-state EEG alpha/theta power ratio discriminates early-onset Alzheimer's disease from healthy controls. Clin Neurophysiol 2021; 132(9): 2019-31. http://dx.doi.org/10.1016/j.clinph.2021.05.012 PMID: 34284236

[7] Serrano-Pozo A, Frosch MP, Masliah E, Hyman BT. Neuropathological alterations in Alzheimer disease. Cold Spring Harb Perspect Med 2011; 1(1): a006189. http://dx.doi.org/10.1101/cshperspect.a006189 PMID: 22229116

[8] Stomrud E, Hansson O, Minthon L, Blennow K, Rosén I, Londos E. Slowing of EEG correlates with CSF biomarkers and reduced cognitive speed in elderly with normal cognition over 4 years. Neurobiol Aging 2010; 31(2): 215-23. http://dx.doi.org/10.1016/j.neurobiolaging.2008.03.025 PMID: 18462837

[9] Leuzy A, Smith R, Cullen NC, *et al.* Biomarker-based prediction of longitudinal tau positron emission tomography in alzheimer disease. JAMA Neurol 2022; 79(2): 149-58. http://dx.doi.org/10.1001/jamaneurol.2021.4654 PMID: 34928318

[10] Schierle GSK, Michel CH, Gasparini L. Advanced imaging of tau pathology in Alzheimer Disease: New perspectives from super resolution microscopy and label-free nanoscopy. Microsc Res Tech 2016; 79(8): 677-83. http://dx.doi.org/10.1002/jemt.22698 PMID: 27324149

[11] Mantzavinos V, Alexiou A. Biomarkers for alzheimer's disease diagnosis. Curr Alzheimer Res 2017; 14(11): 1149-54. PMID: 28164766

[12] Manyevitch R, Protas M, Scarpiello S, *et al.* Evaluation of metabolic and synaptic dysfunction hypotheses of alzheimer's disease (ad): A meta-analysis of csf markers. Curr Alzheimer Res 2018; 15(2): 164-81. http://dx.doi.org/10.2174/1567205014666170921122458 PMID: 28933272

[13] Schindler SE, Bollinger JG, Ovod V, *et al.* High-precision plasma β-amyloid 42/40 predicts current and future brain amyloidosis. Neurology 2019; 93(17): e1647-59. http://dx.doi.org/10.1212/WNL.0000000000008081 PMID: 31371569

[14] Gao F, Lv X, Dai L, *et al.* A combination model of AD biomarkers revealed by machine learning precisely predicts Alzheimer's dementia: China Aging and Neurodegenerative Initiative (CANDI) study. Alzheimers Dement 2022; alz.12700. http://dx.doi.org/10.1002/alz.12700 PMID: 35668045

[15] Giuliano Zippo A, Castiglioni I. Integration of (18)fdg-pet metabolic and functional connectomes in the early diagnosis and prognosis of the alzheimer's disease. Curr Alzheimer Res 2016; 13(5): 487-97. http://dx.doi.org/10.2174/1567205013666151116142451 PMID: 26567731

[16] Lee JH, Yang DS, Goulbourne CN, *et al.* Faulty autolysosome acidification in Alzheimer's disease mouse models induces autophagic build-up of Aβ in neurons, yielding senile plaques. Nat Neurosci 2022; 25(6): 688-701. http://dx.doi.org/10.1038/s41593-022-01084-8 PMID: 35654956

[17] Babiloni C, Triggiani AI, Lizio R, *et al.* Classification of single normal and alzheimer's disease individuals from cortical sources of resting state eeg rhythms. Front Neurosci 2016; 10: 47. http://dx.doi.org/10.3389/fnins.2016.00047 PMID: 26941594

[18] van der Hiele K, Vein AA, van der Welle A, *et al.* EEG and MRI correlates of mild cognitive impairment and Alzheimer's disease. Neurobiol Aging 2007; 28(9): 1322-9. http://dx.doi.org/10.1016/j.neurobiolaging.2006.06.006 PMID: 16854500

[19] Briels CT, Stam CJ, Scheltens P, Bruins S, Lues I, Gouw AA. In pursuit of a sensitive EEG functional connectivity outcome measure for clinical trials in Alzheimer's disease. Clin Neurophysiol 2020; 131(1): 88-95. http://dx.doi.org/10.1016/j.clinph.2019.09.014 PMID: 31759193

[20] Dauwels J, Vialatte F, Cichocki A. Diagnosis of Alzheimer's disease from EEG signals: where are we standing? Curr Alzheimer Res 2010; 7(6): 487-505. http://dx.doi.org/10.2174/156720510792231720 PMID: 20455865

[21] Czigler B, Csikós D, Hidasi Z, *et al.* Quantitative EEG in early Alzheimer's disease patients — Power spectrum and complexity features. Int J Psychophysiol 2008; 68(1): 75-80. http://dx.doi.org/10.1016/j.ijpsycho.2007.11.002 PMID: 18093675

[22] Jeong J. EEG dynamics in patients with Alzheimer's disease. Clin Neurophysiol 2004; 115(7): 1490-505. http://dx.doi.org/10.1016/j.clinph.2004.01.001 PMID: 15203050

[23] Smailovic U, Jelic V. Neurophysiological markers of alzheimer's disease: quantitative eeg approach. Neurol Ther 2019; 8(S2)(Suppl. 2): 37-55. http://dx.doi.org/10.1007/s40120-019-00169-0 PMID: 31833023

[24] Babiloni C, Lizio R, Marzano N, *et al.* Brain neural synchronization and functional coupling in Alzheimer's disease as revealed by resting state EEG rhythms. Int J Psychophysiol 2016; 103: 88-102. http://dx.doi.org/10.1016/j.ijpsycho.2015.02.008 PMID: 25660305

[25] Amezquita-Sanchez JP, Mammone N, Morabito FC, Marino S, Adeli H. A novel methodology for automated differential diagnosis of mild cognitive impairment and the Alzheimer's disease using EEG signals. J Neurosci Methods 2019; 322: 88-95. http://dx.doi.org/10.1016/j.jneumeth.2019.04.013 PMID: 31055026

[26] McBride JC, Zhao X, Munro NB, *et al.* Spectral and complexity analysis of scalp EEG characteristics for mild cognitive impairment and early Alzheimer's disease. Comput Methods Programs Biomed 2014; 114(2): 153-63. http://dx.doi.org/10.1016/j.cmpb.2014.01.019 PMID: 24598317

[27] Şeker M, Özbek Y, Yener G, Özerdem MS. Complexity of eeg dynamics for early diagnosis of alzheimer's disease using permutation entropy neuromarker. Comput Methods Programs Biomed 2021; 206: 106116. http://dx.doi.org/10.1016/j.cmpb.2021.106116 PMID: 33957376

[28] Tylová L, Kukal J, Hubata-Vacek V, Vyšata O. Unbiased estimation of permutation entropy in EEG analysis for Alzheimer's disease classification. Biomed Signal Process Control 2018; 39: 424-30. http://dx.doi.org/10.1016/j.bspc.2017.08.012

[29] Yan Y, Zhao A, Ying W, *et al.* Functional connectivity alterations based on the weighted phase lag index: An exploratory electroencephalography study on alzheimer's disease. Curr Alzheimer Res 2021; 18(6): 513-22. http://dx.doi.org/10.2174/1567205018666211001110824 PMID: 34598666

[30] Hatz F, Hardmeier M, Benz N, *et al.* Microstate connectivity alterations in patients with early Alzheimer's disease. Alzheimers Res Ther 2015; 7(1): 78. http://dx.doi.org/10.1186/s13195-015-0163-9 PMID: 26718102

[31] Jeong J, Gore JC, Peterson BS. Mutual information analysis of the EEG in patients with Alzheimer's disease. Clin Neurophysiol 2001; 112(5): 827-35. http://dx.doi.org/10.1016/S1388-2457(01)00513-2 PMID: 11336898

[32] Smailovic U, Koenig T, Laukka EJ, *et al.* EEG time signature in Alzheimer´s disease: Functional brain networks falling apart. Neuroimage Clin 2019; 24: 102046. http://dx.doi.org/10.1016/j.nicl.2019.102046 PMID: 31795039

[33] Leuchter AF, Spar JE, Walter DO, Weiner H. Electroencephalographic spectra and coherence in the diagnosis of Alzheimer's-type and multi-infarct dementia. A pilot study. Arch Gen Psychiatry 1987; 44(11): 993-8. http://dx.doi.org/10.1001/archpsyc.1987.01800230073012 PMID: 3314770

[34] Sandmann MC, Piana ER, Sousa DS, De Bittencourt PR. [Digital EEG with brain mapping in Alzheimer's dementia and Parkinson's disease. A prospective controlled study]. Arq Neuropsiquiatr 1996; 54(1): 50-6. http://dx.doi.org/10.1590/S0004-282X1996000100009 PMID: 8736145

[35] Babiloni C, Del Percio C, Boccardi M, *et al.* Occipital sources of resting-state alpha rhythms are related to local gray matter density in subjects with amnesic mild cognitive impairment and Alzheimer's disease. Neurobiol Aging 2015; 36(2): 556-70. http://dx.doi.org/10.1016/j.neurobiolaging.2014.09.011 PMID: 25442118

[36] Babiloni C, Binetti G, Cassetta E, *et al.* Sources of cortical rhythms change as a function of cognitive impairment in pathological aging: A multicenter study. Clin Neurophysiol 2006; 117(2): 252-68. http://dx.doi.org/10.1016/j.clinph.2005.09.019 PMID: 16377238

[37] van der Hiele K, Vein AA, Reijntjes RHAM, *et al.* EEG correlates in the spectrum of cognitive decline. Clin Neurophysiol 2007; 118(9): 1931-9. http://dx.doi.org/10.1016/j.clinph.2007.05.070 PMID: 17604688

[38] Babiloni C, Frisoni G, Pievani M, *et al.* Hippocampal volume and cortical sources of EEG alpha rhythms in mild cognitive impairment and Alzheimer disease. Neuroimage 2009; 44(1): 123-35. http://dx.doi.org/10.1016/j.neuroimage.2008.08.005 PMID: 18805495

[39] Bennys K, Rondouin G, Vergnes C, Touchon J. Diagnostic value of quantitative EEG in Alzheimer's disease. Neurophysiol Clin 2001; 31(3): 153-60. http://dx.doi.org/10.1016/S0987-7053(01)00254-4 PMID: 11488226

[40] Ponomareva NV, Selesneva ND, Jarikov GA. EEG alterations in subjects at high familial risk for Alzheimer's disease. Neuropsychobiology 2003; 48(3): 152-9. http://dx.doi.org/10.1159/000073633 PMID: 14586166

[41] Benwell CSY, Davila-Pérez P, Fried PJ, *et al.* EEG spectral power abnormalities and their relationship with cognitive dysfunction in patients with Alzheimer's disease and type 2 diabetes. Neurobiol Aging 2020; 85: 83-95. http://dx.doi.org/10.1016/j.neurobiolaging.2019.10.004 PMID: 31727363

[42] Moretti D, Paternicò D, Binetti G, Zanetti O, Frisoni G. EEG upper/low alpha frequency power ratio and the impulsive disorders network in subjects with mild cognitive impairment. Curr Alzheimer Res 2014; 11(2): 192-9. http://dx.doi.org/10.2174/1567205011021403131555546 PMID: 24661147

[43] Polverino P, Ajčević M, Catalan M, Mazzon G, Bertolotti C, Manganotti P. Brain oscillatory patterns in mild cognitive impairment due to Alzheimer's and Parkinson's disease: An exploratory high-density EEG study. Clin Neurophysiol 2022; 138: 1-8. http://dx.doi.org/10.1016/j.clinph.2022.01.136 PMID: 35349920

[44] Koenig T, Prichep L, Dierks T, *et al.* Decreased EEG synchronization in Alzheimer's disease and mild cognitive impairment. Neurobiol Aging 2005; 26(2): 165-71. http://dx.doi.org/10.1016/j.neurobiolaging.2004.03.008 PMID: 15582746

[45] McKhann GM, Knopman DS, Chertkow H, *et al.* The diagnosis of dementia due to Alzheimer's disease: Recommendations from the National Institute on Aging-Alzheimer's Association workgroups on diagnostic guidelines for Alzheimer's disease. Alzheimers Dement 2011; 7(3): 263-9. http://dx.doi.org/10.1016/j.jalz.2011.03.005 PMID: 21514250

[46] Zhang J, Zhang M, Jiang N. Phase average waveform and phase difference analysis of different leads for alzheimer's disease electroencephalograph signals. J Med Imag Health 2018; 8: 1358-63.

[47] Klimesch W. EEG alpha and theta oscillations reflect cognitive and memory performance: A review and analysis. Brain Res Brain Res Rev 1999; 29(2-3): 169-95. http://dx.doi.org/10.1016/S0165-0173(98)00056-3 PMID: 10209231

[48] Babiloni C, Ferri R, Noce G, *et al.* Resting-state electroencephalographic delta rhythms may reflect global cortical arousal in healthy old seniors and patients with Alzheimer's disease dementia. Int J Psychophysiol 2020; 158: 259-70. http://dx.doi.org/10.1016/j.ijpsycho.2020.08.012 PMID: 33080295

[49] Blinowska KJ, Rakowski F, Kaminski M, *et al.* Functional and effective brain connectivity for discrimination between Alzheimer's patients and healthy individuals: A study on resting state EEG rhythms. Clin Neurophysiol 2017; 128(4): 667-80. http://dx.doi.org/10.1016/j.clinph.2016.10.002 PMID: 27836429

[50] Babiloni C, Blinowska K, Bonanni L, *et al.* What electrophysiology tells us about Alzheimer's disease: A window into the synchronization and connectivity of brain neurons. Neurobiol Aging 2020; 85: 58-73. http://dx.doi.org/10.1016/j.neurobiolaging.2019.09.008 PMID: 31739167

[51] Cicalese PA, Li R, Ahmadi MB, *et al.* An EEG-fNIRS hybridization technique in the four-class classification of alzheimer's disease. J Neurosci Methods 2020; 336: 108618. http://dx.doi.org/10.1016/j.jneumeth.2020.108618 PMID: 32045572

[52] Staff RT, Murray AD, Ahearn T, *et al.* Brain volume and survival from age 78 to 85: The contribution of Alzheimer-type magnetic resonance imaging findings. J Am Geriatr Soc 2010; 58(4): 688-95. http://dx.doi.org/10.1111/j.1532-5415.2010.02765.x PMID: 20398148